SC Wall Piers and Basemat Connections: Numerical Investigation of Behavior and Design

Efe G. Kurt[1], Amit Varma[2], Peter Booth[1] and Andrew S. Whittaker[3]

[1]Ph.D. Candidate, Dept. of Civil Engineering, Purdue University, West Lafayette, IN, ekurt@purdue.edu
[2]Associate Professor, Dept. of Civil Engineering, Purdue University, West Lafayette, IN, ahvarma@purdue.edu
[3]Professor and Chair; Director, MCEER; Dept. of Civil, Structural and Environmental Engineering, University at Buffalo, NY

ABSTRACT

This paper presents the development and benchmarking of 3D finite element models for predicting the lateral load (in-plane shear) behavior of SC wall piers and their anchorage to the concrete basemat. The benchmarking is done using the results of selected experimental investigations (tests) from the overall database. The benchmarked models are used to conduct parametric studies, and the results from these studies are used to: (i) evaluate the lateral load-deformation of SC wall piers, and (ii) to develop recommendations for the SC wall-to-basemat anchorage design. Full-strength connection design, which requires the anchorage to be stronger than the wall pier, is recommended for the SC wall-to-basemat anchorage. A potential test matrix is recommended for further verifying the results of the numerical studies presented in this paper.

INTRODUCTION AND OUTLINE

Steel-concrete (SC) composite walls are being used for current safety-related nuclear facilities, and being considered for small modular reactors of the future. There are no approved US codes or standards for the design of SC walls and their connections to the concrete basemat at this time. This paper focuses on the in-plane shear behavior of SC wall piers, and proposes recommendations for anchoring them into the concrete basemat.

The in-plane shear behavior of SC walls has been studied extensively in Japan, Korea, and the US. Experimental investigations have been conducted on SC wall specimens with and without flanges (or boundary elements) in Japan (Funakoshi et al. 1998) and the US (Varma et al. 2011a). In-plane shear tests have been conducted on SC wall panels with or without accident thermal loading (Ozaki et al., 2000). Takeuchi et al. (1998) have also evaluated the behavior of SC walls under axial compression, and under in-plane shear. Experimental investigations of SC wall to basemat connections have been very limited. Fujita et al. (1998) conducted tests on SC walls anchored to the concrete basemat using anchor rods or dowel bars. More recently, researchers in the US (Epackachi et al., 2013) have tested four SC wall pier specimens with different reinforcement ratios, shear stud spacing, and tie bar spacing. The tests focused on the in-plane behavior of SC wall piers, not their anchorage to the concrete basemat.

This paper presents the development and benchmarking of 3D finite element models for predicting the lateral load (in-plane shear) behavior of SC wall piers and their anchorage to the concrete basemat. The benchmarking was done using the results of selected experimental investigations (tests) from the overall database including lateral loading (in-plane shear) tests of SC walls with and without flanges. The benchmarked models were used to investigate the lateral load capacity of SC wall piers without flanges. The parameters included were the wall thickness, the wall aspect (height-to-length) ratio, and steel plate reinforcement ratios. The results from the analytical parametric studies are presented along with insights into the behavior of SC wall piers.

The benchmarked models were used to further investigate behavior and develop recommendations for the SC wall pier-to-concrete basemat anchorage. Full-strength connection design, which requires the

anchorage to be stronger than the SC wall pier, is recommended based on the analysis results because it results in ductility and energy dissipation through yielding and plastification of the SC wall pier. The parametric analyses are used to recommend the relative strength ratio (α) of the anchorage to the SC wall pier to achieve full-strength connection design.

EXPERIMENTAL STUDIES SELECTED FROM THE DATABASE

This section presents relevant details of the tests that were included in the benchmarking analysis of the 3D finite element models. These included tests conducted on SC walls with flanges (Takeuchi et al. 1998) and SC walls without flanges (Epackachi et al. 2013) that were selected from the overall database mentioned earlier.

SC Walls with flanges

The typical configuration of specimens tested by Takeuchi et al. (1998) is shown in Figure 1(a). The bottom portion of the specimen is embedded into a concrete base slab. Another concrete loading slab is located at the top of the specimen. The specimen is subjected to cyclic lateral loading, which is applied using hydraulic actuators connected to the top loading slab. A total of seven in-plane tests were conducted on specimens with varying aspect ratios, wall thickness, and steel plate thicknesses. Three different steel reinforcement ratios, namely 1.3%, 2% and 4 % are used with wall aspect (H/L) ratios of 0.87, 1.09 and 1.53. The specimen wall length (L) was equal to 1660 mm for all the experiments. The wall thicknesses were 4.5 in., 9 in. and 13.5 in. The steel faceplate thickness was equal to 0.09 in. for all the specimens. The steel faceplates were anchored to the concrete infill using headed shear studs at equal horizontal and vertical spacing. The stud spacing was equal to 33 times of web steel plate thickness for all specimens.
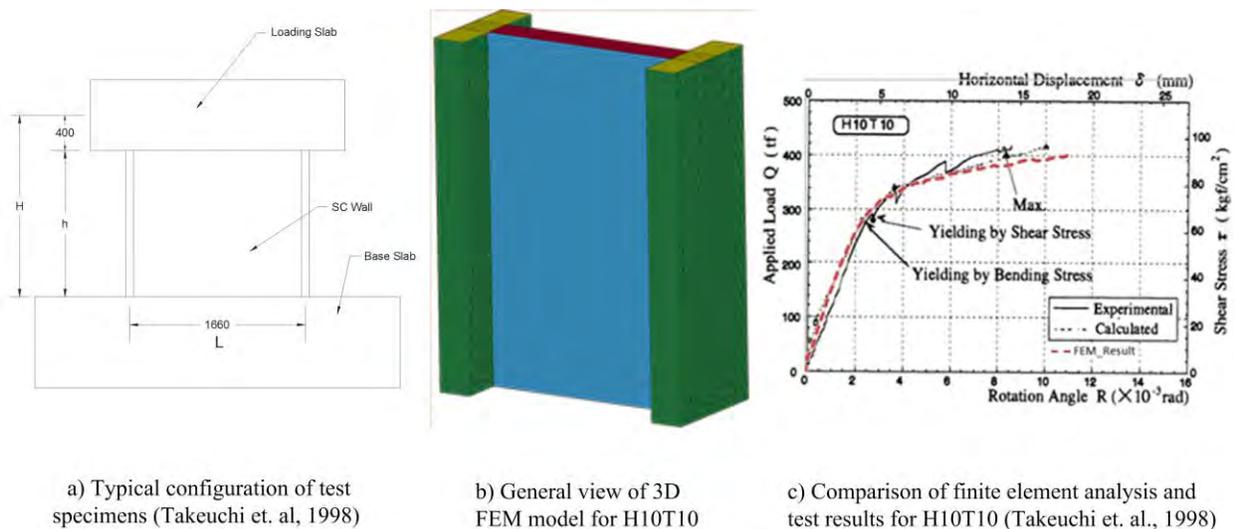

a) Typical configuration of test specimens (Takeuchi et. al, 1998)

b) General view of 3D FEM model for H10T10

c) Comparison of finite element analysis and test results for H10T10 (Takeuchi et. al., 1998)

Figure 1. Typical configuration of test specimens (Takeuchi et. al, 1998)

SC Wall Piers

Epackachi et al (2013) have recently conducted large-scale tests focusing on the in-plane shear behavior of SC wall pier specimens. Figure 2 shows relevant details of the test setup and the specimens. As shown, all the SC wall pier specimens were 72in. in height and 60 in. in length. The steel faceplate thicknesses were equal to 3/16 in for all the specimens. Two different reinforcement ratios of 4.2% and 3.1% were achieved by altering the wall thicknesses of the specimens from 9 in. to 12 in., respectively. The wall height-to-length (H/L) aspect ratio of 1.0 was achieved by applying the lateral loading at a height of 60 in. from the top of the base plate (Figure 2.b). The faceplates were welded to the steel baseplate as shown in Figure 2(c). The spacing of the shear studs was equal to 4 in.
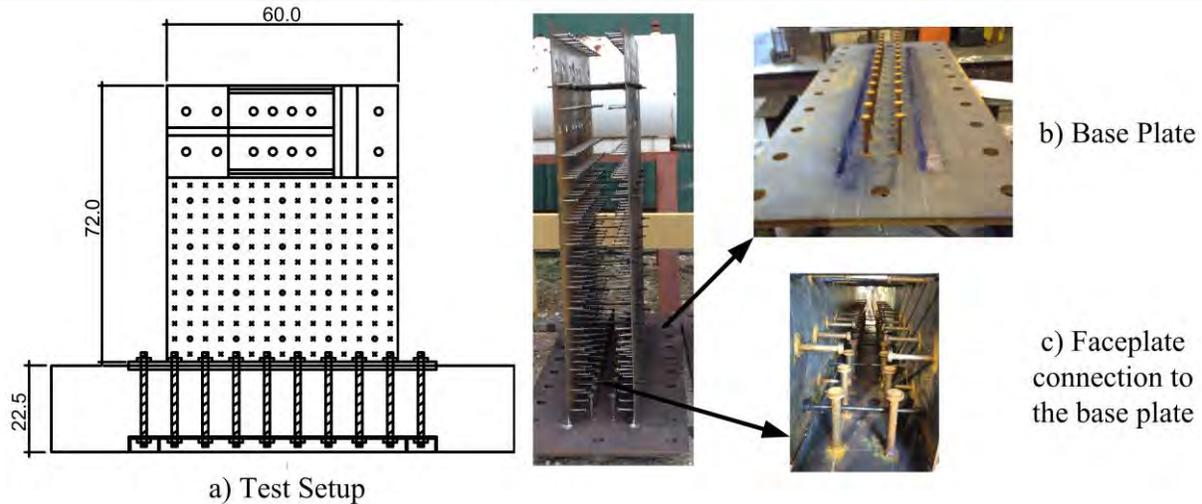
a) Test Setup

b) Base Plate

c) Faceplate connection to the base plate

Figure 2. Test setup and Details of Specimen SC1 tested by Epackachi et al., (2013).

3D FINITE LEMENT MODELS: DEVELOPMENT AND BENCHMARKING

This section presents the development and benchmarking of the 3D finite element models for predicting the in-plane shear behavior of SC walls. The models were developed and analyzed in LS-DYNA, which is a commercially available finite element analysis program. As mentioned earlier, the benchmarking was done for SC walls without flanges tested by Takeuchi et al. (1998) and wall piers without flanges tested by Epackachi et al. (2013). As described in the following sub-sections, the finite element models explicitly modeled the nonlinear inelastic behavior of the steel faceplates, concrete infill, shear studs, and tie rods, and the interaction between them. The anchorage details of the tested specimens were included in the models where available. The following sub-section provides a brief summary and comparison of the results predicted by the finite element models with the experimental results.

SC Walls with flanges

The sub-section describes the model developed for the test denoted as H10T10 by Takeuchi et al. (1998). The model and comparisons presented here are representative and typical for SC walls with flanges tested by Takeuchi et al. (1998). Figure 1(b) shows a rendering of the test specimen, H10T10, from the finite element model in LS-DYNA. As shown, the model explicitly accounted for the SC wall components including the steel plates, concrete infill, and shear studs.

The concrete infill was modeled using eight-node solid elements and the continuous surface cap model referred as CSCM_Concrete in LS-DYNA. The steel plates were modeled 4-node shell elements and the piecewise_linear_plasticity material model in LS-DYNA. The shear studs were modeled using beam elements and the same piecewise_linear_plasticity material model for steel. These beam elements are constrained in the concrete infill by coupling acceleration and velocity using lagrange_in_solid keyword definition.

Figure 1(c) shows the comparison of the lateral load-displacement response predicted by the finite element model and measured experimentally for Specimen H10T10. The lateral load-displacement response compares favorably with experimental measurements with some minor deviations. The initial slope (stiffness) predicted by the finite element model is slightly (5%) higher than the experimental measurements. This is probably due to the fact that the model does not account for locked in shrinkage strains in the concrete infill. The ultimate strength (peak load capacity) predicted by the finite element model compares conservatively with the experimental results. The comparisons shown in Figure 1(c) are

typical and representative of the lateral load-displacement comparisons for the other SC walls with flanges specimens tested by Takeuchi et al. (1998).

SC Wall Piers

The sub-section describes the model developed for the SC wall pier test denoted as Specimen SC1 by Epackachi et al. (2013). The model and comparisons presented here are representative and typical for SC wall piers tested by Epackachi et al. (2013). Figure 3 shows renderings of Specimen SC 1 from the finite element models developed in LS-DYNA. As shown, the model explicitly accounted for the SC wall components including the steel plates, concrete infill, shear studs, tie rods, and their interfacial interactions. Additionally, the model explicitly accounted for the components of the SC wall anchorage including the steel baseplate that the SC wall is welded to, the threaded steel anchor rods, and the concrete foundation post-tensioned to the laboratory strong floor.
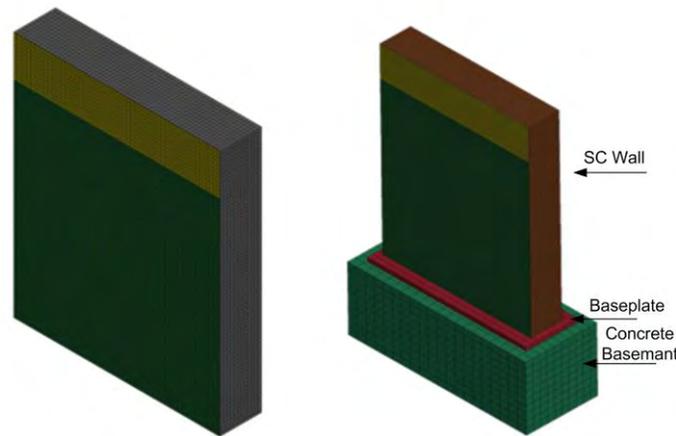

Figure 3. General views of the developed models for SC1 (Epackachi et. al, 2013).

The concrete infill was modeled using eight-node solid elements and the Winfrith concrete model in LS-DYNA. The steel plates were modeled 4-node shell elements and the piecewise_linear_plasticity material model in LS-DYNA. The shear studs and tie rods were modeled using beam elements and the same piecewise_linear_plasticity material model for steel. These beam elements are constrained in the concrete infill by coupling acceleration and velocity using lagrange_in_solid keyword definition. The steel baseplate of the anchorage was modeled using eight-node solid elements and the piecewise_linear_plasticity material model. The anchor rods of the basemat were modeled using beam elements and the same piecewise_linear_plasticity material model for steel. The concrete foundation was modeled using the eight node solid elements and the continuous surface cap model referred as CSCM concrete model in LS-DYNA.

Figure 4 shows the comparison of the lateral load-displacement response predicted by the finite element model and measured experimentally for Specimen SC1. Two models were analyzed: (i) assuming fixity at the base of the SC wall without modeling the anchorage, and (ii) explicitly modeling the SC wall-to-basemat anchorage. As shown in Figure 4, the finite element model with fixed base (no anchorage connection) predicts the peak load capacity reasonably (within 5%), but has much higher initial stiffness than the test data. The finite element model of SC wall with base anchorage predicts both the stiffness and strength of the test specimen with reasonable accuracy. It predicts the peak load capacity within 2% of the test data. This confirms the importance of modeling the basemat anchorage along with the SC wall pier to accurately predict the overall lateral load-deformation behavior.
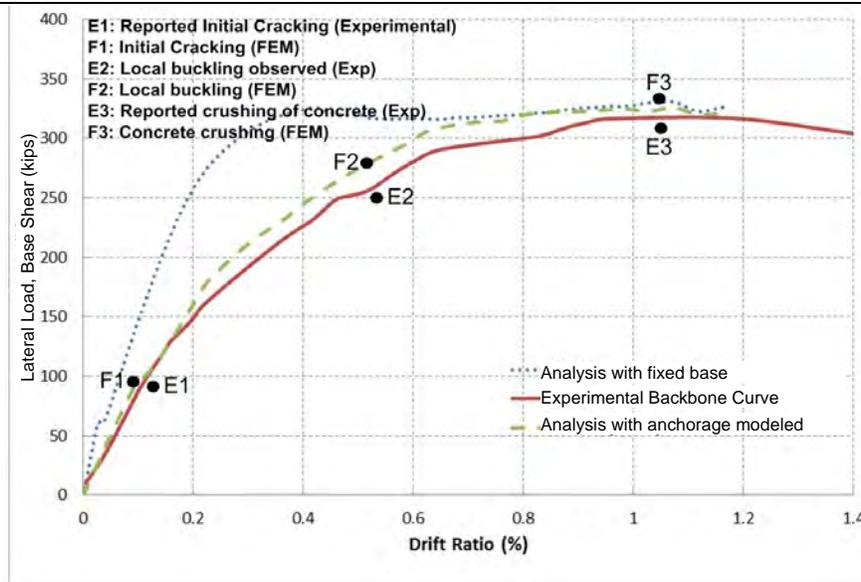
a) Comparison of damage states for SC1

b) Visual comparison of initiation of local buckling (same drift ratio)
Figure 4. Comparison of damage states of the experiment and FEM

Figure 4(a) includes data points indicating the occurrence of events during the experiment and the analysis. As shown the predictions from the finite element model are consistent with those observed during the test. At approximately 0.1% drift ratio, initiation of concrete cracking was observed both in the test and analysis. At approximately 0.5% drift ratio, local buckling of the steel faceplates occurred in both the test and the analysis. Figure 4(b) shows photographs of local buckling observed during the test, and local buckling predicted by the finite element model. At approximately 1% drift ratio, crushing of the concrete in compression occurred in both the test and the analysis. The comparisons shown in Figure 4 are typical and representative of the lateral load-displacement comparisons for the other SC walls pier specimens tested by Epackachi et al. (2013)

LATERAL LOAD CAPACITY OF SC WALL PIERS

The benchmarked finite element models were used to investigate the lateral load capacity of SC wall piers, and conduct parametric studies. The parameters included were: (i) the SC wall thickness (T), (ii) the wall pier height-to-length (H/L) aspect ratio, and (iii) the steel faceplate reinforcement ratio ($2t_p/T$). Three different wall thickness values (T = 9, 12, and 18 in. were considered). Six different wall aspect ratios (H/L = 0.5, 0.6, 0.75, 1.5, and 3.0) were considered, and three different reinforcement ratios (2.0%, 3.1%, and 4.2%) were considered. The parameters that were not changed during the investigations were the steel faceplate yield stress (F_y = 36 ksi), the concrete compressive strength (f'_c = 4400 psi), and the steel faceplate slenderness ratio (stud spacing to plate thickness s/t_p ratio = 21).

The results from the parametric analyses are shown in Figure 5. It includes the lateral load-deformation responses of SC wall piers with thickness equal to 12 in., reinforcement ratio equal to 3.1%, and with different aspect ratios (H/L = 0.5 to 3.0). Figure 5(a) shows plots of the base shear – interstory drift ratios, and Figure 5(b) shows plots of the base moment – interstory drift ratios. The behavior in Figure 5(a) shows that the lateral load capacity (and the base shear) increases as the wall aspect ratio decreases from 3 to 0.5. The behavior in Figure 5(b) shows that the as the wall aspect ratio increases from 0.5 to 3.0, the base moment corresponding to the lateral load capacity increases.

The variations shown in Figure 5(a) and (b) are expected for wall piers with different aspect (H/L) ratios. Figure 5(a) includes a horizontal line corresponding to the pure in-plane shear strength (A_sF_y) of the corresponding SC wall panels (not pier) subjected to pure in-plane shear loading only. This pure in-plane shear strength of SC wall panels was discussed extensively by Varma et al. (2011b), and calculated as βA_sF_y, which is based on the cracked orthotropic composite interaction between the steel plates and the concrete infill. The value of β was approximately equal to 1.0 for reinforcement ratio equal to 3.1%.

Figure 5(a) shows that the SC wall pier base shear increases with decreasing aspect ratios (H/L) but does not reach the pure in-plane shear strength (A_sF_y) of SC wall panels because SC wall piers are not subjected to pure in-plane shear loading in the analyses. As shown in Figure 5(b), they are subjected to flexural moments at the base (M_{base}) in addition to the base shear (V_{base}). Figure 5(b) includes a horizontal line corresponding to the flexural capacity (M_n) of the cross-section at the base of the SC wall pier. This flexural capacity (M_n) was calculated using a fiber analysis of the cross-section, while assuming strain compatibility between the steel and concrete, maximum concrete compressive strain equal to 0.003, Hognestad's uniaxial stress-strain curve for the concrete, and elastic-plastic stress-strain curve for the steel. As shown in Figure 5(b) SC wall piers with aspect ratios greater or equal to 1.0 develop the flexural capacity (M_n) of the wall cross-section at the base.

In summary, Figures 5(a) and (b) shows that SC wall piers reach their lateral load capacity due to combined in-plane flexure (M_{base}) and shear (V_{base}). The lateral load capacity of SC wall piers with aspect ratios greater than or equal to 1 is governed by the flexural capacity (M_n) of the SC cross-section at the base of the wall. The lateral load capacity of SC wall piers with aspect ratios less than 1.0 is governed by shear failure of the wall base, but it never reaches the pure in-plane shear strength of SC wall panels.

Similar analyses were conducted for SC wall piers with wall thickness of 9 in. (reinforcement ratio = 4.2%) and 18 in. (reinforcement ratio = 2.0%). Figure 6 summarizes the results from all the parametric analyses of SC wall piers. For each wall thickness (T=9, 12, and 18 in.), Figure 6 presents the normalized lateral load capacity as a function of the wall aspect (H/L) ratio. Each of the Figures 6(a), (b), and (c) includes: (i) the lateral load capacity or base shear (V_{base}) normalized with respect to AsFy, which represents the pure in-plane shear strength of SC panels, and (ii) the moment at the base (Mbase) corresponding to the lateral load capacity normalized with respect to the flexural moment capacity M_n, which represents the calculated moment capacity of SC base cross-section.

The results in Figure 6 show that the lateral load capacity and associated base shear (V_{base}) increases and approaches the in-plane shear capacity (A_sF_y) of the SC wall panel as the wall aspect (H/L) ratio decreases. The lateral load capacity decreases as the wall aspect (H/L) ratio increases, but the associated base moment (M_{base}) reaches the flexural moment capacity (M_n) of the SC base cross-section. The base moment (M_{base}) reaches the flexural moment capacity (M_n) of SC Wall cross section at aprroximately H/L = 3.0.

SC WALL PIER-TO-CONCRET BASEMAT ANCHORAGE DESIGN

The full-strength connection design philosophy consists of: (i) designing the connections to be stronger than the weaker of the two connected parts, and (ii) detailing the connected parts to have ductile failure modes (limit states) with good energy dissipation. Full-strength connection design provides good ductility and energy dissipation under seismic loading by concentrating inelasticity in the weaker of the connected parts, while the connection remains essentially elastic with some localized yielding.
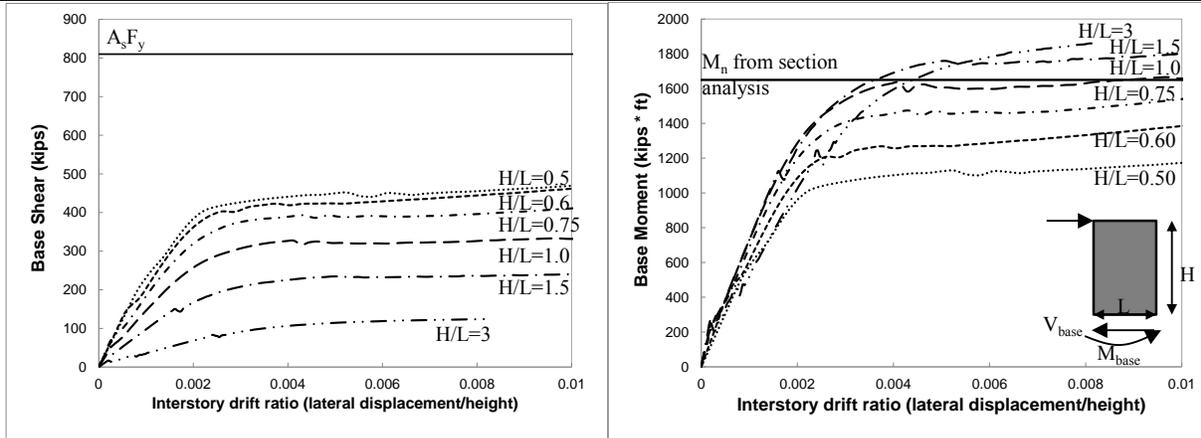
Figure 5. Results from Lateral Load – Deformation Analysis of SC Wall Piers: (a) Base Shear vs. Interstory drift ratio, (b) Base Moment vs. Interstory drift ratio
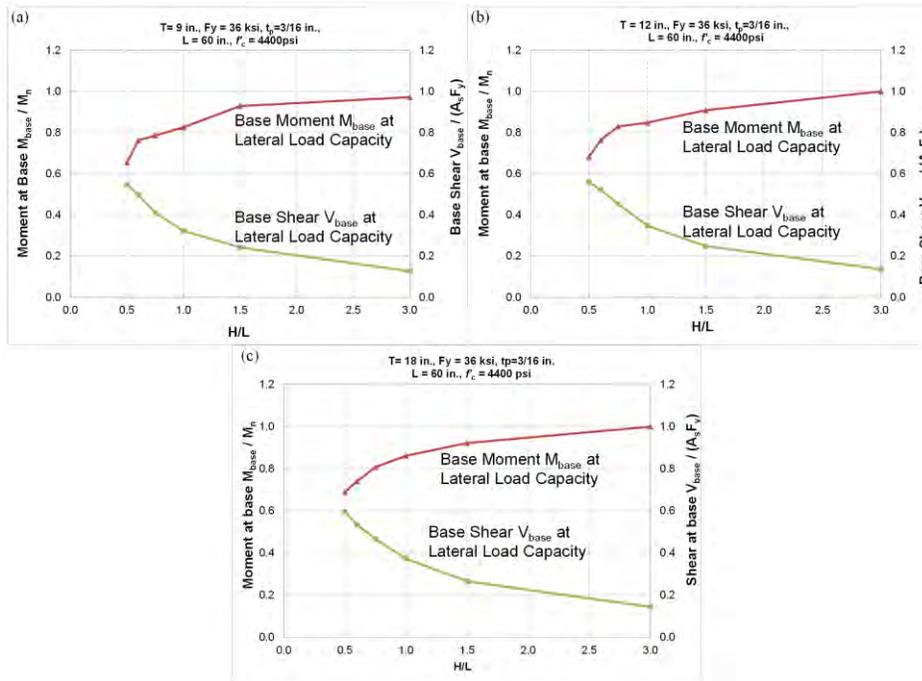

Figure 6. Results from Parametric Analyses of Lateral Load Capacity of SC Wall Piers:
(a) Wall Thickness = 9 in., (b) Wall Thickness = 12 in., (c) Wall Thickness = 18 in.

Full-strength connection design is recommended for SC wall pier-to-basemat anchorage systems so that the lateral load behavior, strength, and ductility are governed by the SC wall pier rather than the basemat anchorage. Analytical parametric studies were conducted using the benchmarked models to develop the full strength design approach for SC wall-to-basemat anchorage connections as follows.

The tensile strength (ϕR_n^{anch}) of the anchorage connection can be calculated using Equation (1). In this equation, A_{sc} and f_{uta} are the cross-sectional area and tensile strength of anchor rods, and n is the number of anchor rods under the wall pier. The yield strength (ϕR_n^{SC}) of the SC walls in tension can be calculated using Equation (2), in which A_s and F_y are the cross-sectional area and yield strength of the steel faceplates of the SC wall pier. As shown in Equation 3, the parameter α is defined as the relative strength ratio of the of the tensile strength (ϕR_n^{anch}) of the anchorage connection to the yield strength (ϕR_n^{SC}) of the SC wall pier in tension.

$$\phi R_n^{anch} = n \text{ x } A_{sc} \text{ x} f_{uta} \tag{1}$$

$$\phi R_n^{SC} = A_s \text{ x} f_y \tag{2}$$

$$\alpha = \phi R_n^{anch} / \phi R_n^{SC} = n \text{ x } A_{sc} \text{ x } f_{uta} / A_s \text{ x } f_y \tag{3}$$

The parametric studies were conducted to investigate the effects of the relative tensile strength ratio (parameter α) on the lateral load behavior of the SC wall pier-to-basemat anchorage system, and the minimum value of the parameter needed to develop full-strength connection behavior. Figure 7 shows the typical SC wall-to-basemat anchorage, and the range of α-values considered in this study. As shown, the SC wall pier is welded to a steel baseplate, and the baseplate is anchored to concrete foundation using J-bolt anchors. The yield and ultimate strengths of the bolt anchors are selected to be 60 and 80 ksi, respectively. The range of α-values considered in the study is equal to 0.25-to-1.25 in increments of 0.25. The study focused on wall piers with thickness (T) equal to 12 in., and three different wall aspect (H/L) ratios were considered with values equal to 0.60, 0.75, and 1.0.

The nonlinear inelastic finite element models were similar to those developed and benchmarked earlier. Additionally, the steel baseplate and the J-bolts were modeled individually. The J-bolts were modeled using Hughes-Liu beam elements in LS-DYNA. Hughes-Liu element type is a simple and computationally efficient beam element type that is compatible with brick elements as it is based on a degenerated brick element formulation (Hallquist, 2006). It also includes finite transverse shear strains. Several beam elements were used to model each J-bolt, and the length of each element was equal to 1.5 times the bolt diameter. These J-bolt elements were embedded in the concrete elements of the basemat by constraint type lagrange_in_solid. The concrete basemat was modeled using the eight node solid elements and the continuous surface cap model referred as CSCM concrete model in LS-DYNA.

The concrete infill was modeled using eight-node solid elements and the Winfrith concrete model in LS-DYNA. The steel plates were modeled 4-node shell elements and the piecewise_linear_plasticity material model in LS-DYNA. The shear studs and tie rods were modeled using beam elements and the same piecewise_linear_plasticity material model for steel.

Figure 8 shows the results from the analyses of the SC wall pier-to-basemat anchorage with wall height-to-length (H/L) aspect ratio equal to 1.0. The figures includes the lateral load-displacement responses for models with relative tensile strength ratios (α) ranging from 0.25 – 1.25. The lateral load capacity ($V_n^{SC\&anch}$) is normalized with respect to the lateral load capacity (V_n^{SC}) of the SC wall pier (with H/L=1.0) from Figure 6(b). As shown, the SC wall pier-to-basemat anchorage system can develop the full strength (lateral load capacity) of the SC wall pier when the relative tensile strength ratio (α) exceeds 1.0. Failures occur in the basemat anchorage when the relative tensile strength ratio is less than 1.0.

Similar analyses were conducted on SC wall pier-to-basemat anchorage systems with wall height-to-length (H/L) aspect ratios equal to 0.6 and 0.75. The analyses were conducted for anchorage systems with relative tensile strength ratios (α) ranging from 0.25 – 1.25. The ratios of the lateral load capacity ($V_n^{SC\&anch}$) of the wall-anchorage system to the lateral load capacity (V_n^{SC}) of the wall pier alone (taken from Figure 6(b)) are presented in Table 1 below. As shown, SC wall pier-to-basemat anchorage systems can develop the full strength (lateral load capacity) of the SC wall pier when the relative tensile strength ratio exceeds 1.0.

DESIGN RECOMMENDATION AND EXPERIMENTAL VERIFICATION

The results from the parametric analyses were used to develop a simple design recommendation for the SC wall pier-to-basemat anchorage system. Full-strength connection design can be achieved using Equation 4, which requires the factored tensile strength (ϕR_n^{anch}) of the anchorage system to be greater than or equal to α times the expected yield strength of the SC wall pier. The value of α in Equation 4 can be equal to or greater than 1.1. The R_y factor is based on the ratio of the expected-to-nominal yield strength of the steel faceplates of the SC walls, and can be obtained for different plate materials from

ASCE 41-06 (ASCE, 2007). Thus, Equation 4 incorporates the relative tensile strength ratio ($\alpha \geq 1.1$), and additional factors to account for the expected strength of the steel faceplates (R_y) and the resistance factor (ϕ) for the anchorage.

$$\phi \sum A_{s,anchor} \ F_{u,anchor} \geq \alpha \ R_y \ A_{s,faceplate} \ F_{y,faceplate} \tag{4}$$
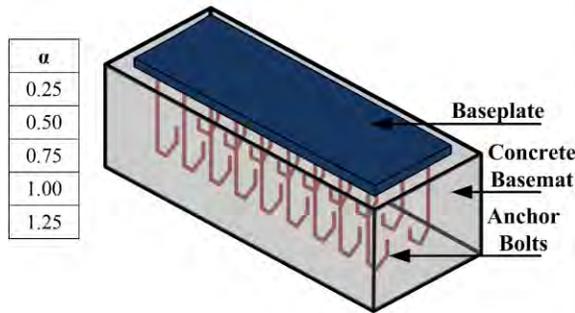

Figure 7. SC Wall Pier to Basemat Anchorage Showing Steel Baseplate and J-bolt anchors.
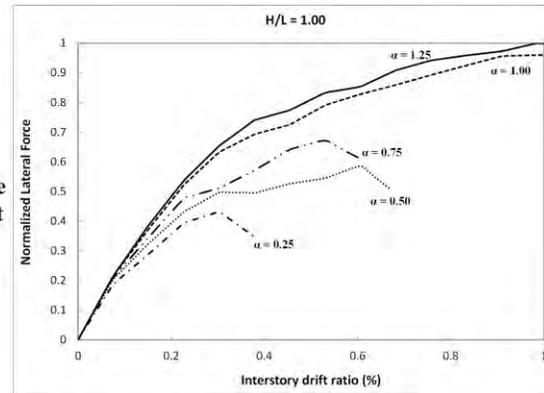

Figure 8. Analysis of SC wall Pier-to-Basemat Anchorage Models with Different Relative α

Table 1. $V_n^{SC+anch}/V_n^{SC}$ Ratios for SC Wall-to-Basemat Anchorage Systems with Different Aspect (H/L) Ratios and Relative Tensile Strength Ratios (α)

Relative Tensile Strength Ratio (α)	Ratio of $V_n^{SC\&anch}/V_n^{SC}$ for H/L = 1.0	Ratio of $V_n^{SC\&anch}/V_n^{SC}$ for H/L = 0.75	Ratio of $V_n^{SC\&anch}/V_n^{SC}$ for H/L = 0.6
0.25	0.43	0.45	0.41
0.50	0.59	0.65	0.64
0.75	0.68	0.82	0.79
1.00	0.96	0.97	0.90
1.25	1.00	1.00	1.00

Test Matrix

Table 2 presents a tentative test matrix of SC wall pier-to-basemat anchorage specimens designed to verify the findings of the numerical investigations and parametric analyses presented in this paper. In Table 2, H, L, T, A$_s$ are the height, length, thickness, and steel faceplate area of the SC wall pier. The matrix includes three specimens with two different H/L ratios (0.60 and 0.75) and three different relative strength ratios ($\alpha = 0.5$, 0.75 and 1.1).

Table 2. Tentative Test Matrix to Confirm Results from Analytical Investigations

Specimen No.	Height H (in.)	Height / Length (H/L)	Length / Wall Thickness (L/T)	Steel Faceplate Area (in^2) (A$_s$)	Tensile Strength Ratio (α)	Expected Failure Location
1	60	0.60	5	22.5	0.5	Connection
2	60	0.60	5	22.5	0.75	Connection
3	60	0.60	5	22.5	1.1	Wall
4	60	0.75	5	22.5	1.1	Wall

As shown in Table 2, Specimen number 1 is designed to fail in the anchorage (not wall pier) with H/L =0.6, α = 0.5. Specimen number 2 is also designed to fail in the anchorage with H/L =0.6, α = 0.75. These results will be used to verify or improve the results of the analytical investigations presented in this

paper. Specimen numbers 3 and 4 are designed to have full-strength anchorage connections, and fail in the SC wall pier with H/L = 0.60 and 0.75 and α = 1.1

CONCLUSIONS

This paper presented the development and benchmarking of 3D finite element models for predicting the lateral load (in-plane shear) behavior of SC wall piers and their anchorage to the concrete basemat. The benchmarked models were used to conduct parametric studies to evaluate the lateral load capacity of SC wall piers with different height-to-length (H/L) aspect ratios and wall thickness. The results indicate that as the wall aspect ratio increases above 1.0, the lateral load capacity is governed by the moment capacity of the cross-section at the base of the wall. The lateral load capacity of wall piers increases with decreasing aspect (H/L) ratios, but it never reaches the pure in-plane shear strength of SC wall panels. The models were used to conduct additional parametric studies to evaluate the lateral load capacity of SC wall pier-to-basemat anchorage systems with: (i) different aspect (H/L) ratios, and (ii) relative tensile strength ratios (α) for the anchorage connection to the SC wall pier. The results indicate that the SC wall pier-to-basemat anchorage systems can develop the full strength (lateral load capacity) of the SC wall pier when the relative tensile strength ratio (α) exceeds 1.0. The results from the analytical studies are used to develop: (i) a simple recommendation to achieve full-strength connection design, and (ii) a tentative test matrix to verify the findings from these analytical studies

References

ASCE, "Seismic Rehabilitation of Existing Buildings (ASCE/SEI 41-06)". American Society of Civil Engineers, 2007.

Epackachi, S., Nguyen, N. H., Kurt, E. G., Whittaker, A. S., and Varma, A.H. "An experimental study of the in-plane shear response of steel concrete composite walls." Trans. of the Internal Assoc. for Struct. Mech. in Reactor Tech.Conf.,, SMiRT-22, San Francisco, USA, Aug. 2013.

Funakoshi, A., Akita, S., Matsumoto, H., Hara, K., Matsuo, I., and Hayashi, N. Experimental study on a concrete filled steel structure Part. 7 Bending Shear Tests (Outline of the experimental program and the results), Summaries of Technical Papers of Annual Meeting, Architectural Institute of Japan, 1998, pp. 1063-1064.

Fujita, T., Funakoshi, A., Akita, S., Hayashi, N., Matsuo, I., and Yamaya, H. Experimental study on a concrete filled steel structure Part. 16 Bending Shear Tests (Effect of Bending Strength), Summaries of Technical Papers of Annual Meeting, Architectural Institute of Japan, 1998, pp. 1125-1126.

Hallquist, J. "LS-Dyna Theory Manual", 2006. <http://www.dynasupport.com/manuals/additional/ls-dyna-theory-manual-2005-beta/at_download/file >.

Ozaki, M., S.Akita, Takeuchi, M., Osuga, H., Nakayama, T., and Niwa, H. Experimental study on a concrete filled steel structure Part. 41 Heating Tests (Outline of the experimental program and the results), Summaries of Technical Papers of Annual Meeting, Architectural Institute of Japan, 2000, pp. 1127-1128

Takeuchi, M., Narikawa, M., Matsuo, I., Hara, K. and Usami, S., "Study on a concrete filled structure for nuclear power plants", Nuclear Engineering and Design, 179, 1998, pp. 209-223.

Varma, A. H., Malushte, S. R., Sener, K., Lai, Z. (2011a). "Steel-plate composite (SC) walls for safety related nuclear facilities: design for in-plane and out-of-plane demands," *Proceedings of the 21st IASMiRT Conference (SMiRT 21)*, New Delhi, India, Paper ID #760.

Varma, A.H., Zhang, K., Chi, H., Booth, P. and Baker, T. (2011b). "In-plane shear behavior of SC composite walls: theory vs. experiment," *Proceedings of the 21st IASMiRT Conference (SMiRT 21)*, New Delhi, India, Paper ID #764.